New Mechanisms for Dissociative Recombination

Steven L. Guberman

*Institute for Scientific Research, 33 Bedford St., Suite 19A, Lexington, MA 02173,
USA*

Three important mechanisms for the dissociative recombination of
an electron with a molecular ion are discussed and each is illustrated
with the results of recent calculations. The mechanisms include direct
capture by derivative coupling for ion and neutral curves which do not
cross, capture by the second order electronic coupling to the interme-
diate vibrationally excited Rydberg states for a crossing of ion and
neutral curves, and dissociative recombination through intermediate
bound excited core Rydberg states.

INTRODUCTION

Much of our understanding of dissociative recombination (DR) has been
based upon the pioneering papers of Bates (1) and Bardsley (2,3), who intro-
duced the direct and indirect DR mechanisms respectively. In recent years
there have been considerable advances in both the theoretical and the labora-
tory methods that are used to study DR. These advances have uncovered new
mechanisms which supplement the earlier mechanisms. In the next section
the highlights of the Bates and Bardsley mechanisms are reviewed. This is
followed by discussions of DR in the case where there is no crossing of ion
and dissociative states, of the second order electronic coupling, and finally of
recombination through a bound excited core Rydberg state.

DIRECT AND INDIRECT DISSOCIATIVE RECOMBINATION

The mechanism for direct dissociative recombination was first described
over 40 years ago by Sir David Bates. (1) In direct dissociative recombination,

$$AB^+ + e^- \rightarrow AB^* \rightarrow A + B, \tag{1}$$
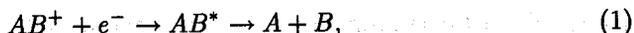
the reactant ion AB^+ captures an electron, e^-, into an electronically excited
state of the neutral molecule, AB^*, which dissociates into the products, A
and B. If AB^+ is a diatomic, A and B can be ground or excited state
atoms. The mechanism for Eq. (1) is illustrated in Fig. (1) where an electron
with energy ϵ is captured directly into a dissociative state. After capture, the
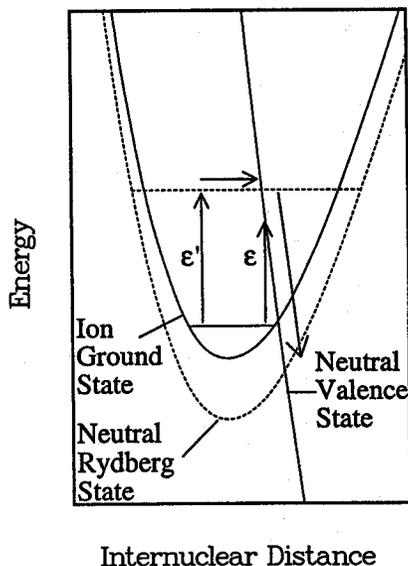molecule may emit an electron leaving the ion in the ground or a vibrationally

Internuclear Distance

FIG. 1. The direct and vibronic indirect dissociative recombination mechanisms.

excited state. On the other hand, if the potential curve is steep and if the autoionization lifetime is longer than the dissociative lifetime, DR is likely. Once the fragments separate beyond the ion potential curve, autoionization is no longer possible. The dissociative states are diabatic states which cross through an infinite number of Rydberg states in order to cross the ion. The matrix element that couples the reactants to the products is over the total Hamiltonian, $H^{Total} = H + T$, where H is the electronic Hamiltonian and T is the nuclear kinetic energy. Because the states are diabatic and do not change character with R, the contribution from T (see Eq. (4)) is negligible compared to that from H. The matrix element over H is given by

$$V_{v,d}^{k,\ell} = \langle \Psi_d X_d \mid H \mid \Psi^{k,\ell} X_v \rangle \tag{2}$$

where Ψ_d and X_d are the electronic and vibrational continuum wave functions, respectively, for the dissociative state. $\Psi^{k,\ell}$ is the electronic wave function for both the ion and the free electron with wave number k and angular momentum, ℓ. X_v is the bound ion vibrational wave function. The direct cross section for DR is approximately proportional to the square of $V_{v,d}^{k,\ell}$. (2,4)

In the indirect recombination mechanism, first proposed by Bardsley (3), the electron is captured into a Rydberg state of the neutral molecule which is predissociated by the repulsive state of the direct mechanism. The indirect mechanism is illustrated in Fig. (1) for capture of an electron with energy ϵ'. The coupling matrix element which drives the capture into the Rydberg vibrational level is again given by a matrix element of the total Hamiltonian, $H^{Total} = H + T$. The matrix element over H vanishes and we are left with

$$T_{v,v',\ell,\ell'}^{n^*,k} = \langle \Psi^{n^*,\ell'} X_v \mid T \mid \Psi^{k,\ell} X_{v'} \rangle \qquad (3)$$

where the wave functions are the same as in Eq. (2) except that now $\Psi^{n^*,\ell'}$ is the electronic wave function of the Rydberg level with effective principal quantum number, n^*. The set of vibrational wave functions for the Rydberg levels is taken to be the same as the set for the ion. The matrix element over the electronic Hamiltonian is zero since the Rydberg states and the free electron states, both with the same ion core, comprise the same spectrum of states that diagonalize the electronic Hamiltonian. This matrix element falls off as $(1/n^*)^{3/2}$ and favors transitions between ion and Rydberg vibrational levels that differ by a single quantum. Bardsley (3) showed that the indirect DR cross section took a Breit-Wigner form in which the resonances contribute peaks to the DR cross section. In this approach, indirect recombination is treated separately from and not allowed to interfere with direct recombination. In the Multichannel Quantum Defect Theory (MQDT) approach to DR introduced by Giusti, (4) this interference is included and it has been shown (4,5) that the cross section near the resonance energy may take the form of a peak (constructive interference), a dip (destructive interference), or a peak on one side of the resonance center and a dip on the other. The shape is determined from the relative magnitudes of the direct recombination matrix element (Eq. (2)) and the matrix elements for the interaction of the Rydberg level with the electron ion continuum (Eq. (3)) and with the dissociative state. (5,6) The resonances take the same form as that predicted by Fano for resonances seen in atomic photoionization. (7)

DISSOCIATIVE RECOMBINATION WITHOUT A CURVE CROSSING

If we shift the repulsive curve in Fig. (1) to smaller R so that it does not cross the ion at all, we would expect the DR cross section to be small because of the small vibrational wave function overlap that enters the matrix element in Eq. (2). Molecules that exhibit this lack of a crossing include the rare gas hydrides and H_3^+. Potential curves calculated (8,9) for HeH are shown in Fig. (2). These curves have been calculated with large Gaussian basis sets and multireference configuration interaction (CI) wave functions. In this system, the dissociative curve equivalent to the repulsive curve of Fig. (1) is the ground state which, however, does not cross the ion. The only remaining dissociative routes are the A and C Rydberg levels which have asymptotes below the v=0 level of the ion. (We neglect the $B^2\Pi$ state because its rotational couplings to the electron-ion state are small.) Because these Rydberg states have the same core as the ion ground state, they too do not cross the ion. Despite this theoretical evidence that might lead one to the conclusion that the HeH DR rate constant may be small, recent experimental results for both $^3HeH^+$ (10,11) and $^4HeH^+$ (12,13) indicate that the cross sections are not negligible.
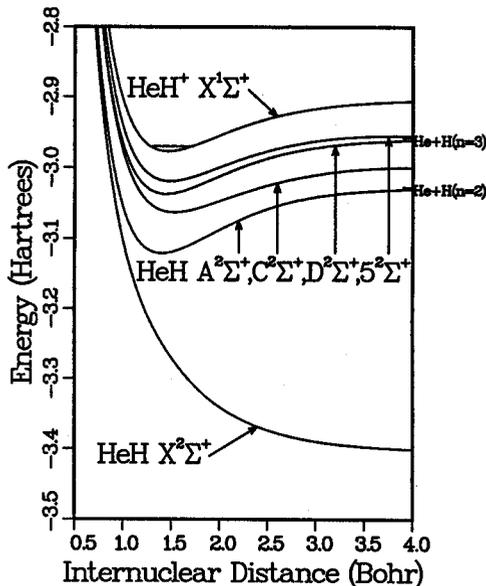
FIG. 2. The calculated potential curves for HeH.

Indeed, a nonnegligible cross section can occur in the absence of a crossing if a new mechanism is introduced in which the electron capture into the dissociative state is driven by the nuclear kinetic energy operator, (8) the same operator that drives the Bardsley indirect capture mechanism. Because this matrix element is nonzero between electron-ion and Rydberg states with the same core, it can drive direct DR along the Rydberg A and C states shown in Fig. (2). In order to calculate DR cross sections and rates, we have included these matrix elements in a revised version of the first order MQDT of Giusti. (4)

For the cross section calculations, we must determine matrix elements over the nuclear kinetic energy operator,

$$T = \frac{-\hbar^2}{2\mu} \frac{1}{R^2} \frac{\partial}{\partial R} R^2 \frac{\partial}{\partial R}, \tag{4}$$

where R is the internuclear distance, $\hbar$ is Planck's constant, and μ is the reduced mass. The matrix element over T reduces to

$$T_{v,d}^{k,\ell} = \rho^{\frac{1}{2}} \langle \Psi_d X_d \mid T \mid \Psi^\ell X_v \rangle = \rho^{\frac{1}{2}} \frac{-\hbar^2}{2\mu} \langle X_d \mid B_d^\ell(R) + 2A_d^\ell(R) \frac{\partial}{\partial R} \mid X_v \rangle, \tag{5}$$

where

$$A_d^\ell(R) = \langle \Psi_d \mid \frac{\partial}{\partial R} \mid \Psi^\ell \rangle, \tag{6}$$

$$B_d^\ell(R) = \langle \Psi_d \mid \frac{\partial^2}{\partial R^2} \mid \Psi^\ell \rangle, \tag{7}$$

310

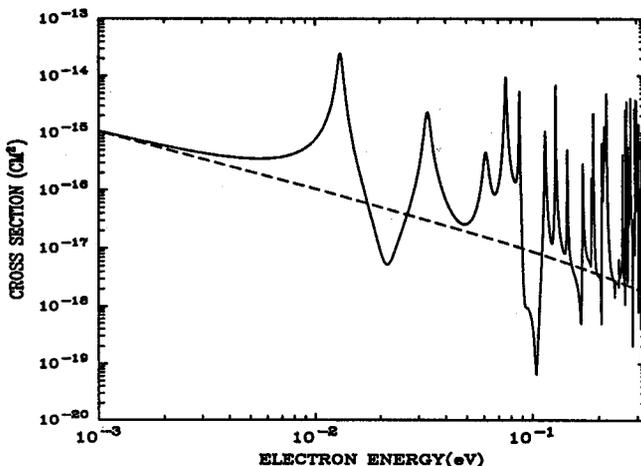**FIG. 3.** Calculated cross sections for DR of $^4HeH^+$.

and ρ is a density of states which converts the matrix elements to those appropriate for an electron-ion continuum. (8,9) The k superscript has been dropped on the right side of Eqs. (5-7) because the matrix elements are calculated for zero energy electrons. Matrix elements of $A_d^\ell(R)$ between the neutral HeH states have already been reported in the literature (14) as have the $\langle \frac{\partial \Psi_d}{\partial R} \mid \frac{\partial \Psi^\ell}{\partial R} \rangle$ matrix elements. (14) The $B_d^\ell(R)$ matrix elements can be derived from these matrix elements by using

$$B_d^\ell(R) = \frac{\partial A_d^\ell}{\partial R} - \langle \frac{\partial \Psi_d}{\partial R} \mid \frac{\partial \Psi^\ell}{\partial R} \rangle. \tag{8}$$

Denoting the Rydberg orbitals by (n, ℓ), the A and C Rydberg states have an electron in the (2,0) and (2,1) Rydberg orbitals respectively. The published couplings (14) show that the strongest interaction is for the capture of an $\ell = 0$ electron into the C state, i.e. a $\Delta\ell = 1$ transition. Furthermore, because the C state is the closest dissociative state to the ion, it has the largest nuclear wave function overlap contribution to the matrix elements in Eq. (5).

We have calculated DR cross sections for $^4HeH^+$ and these are shown in Fig. (3). For $^4HeH^+$, ten bound vibrational levels were included in the first order MQDT calculations. The direct cross section is shown by the dashed line. The direct DR cross sections are small compared to those for many molecules that have favorable diabatic curve crossings. The direct rate at 300K derived from this direct cross section is $4.2x10^{-10}cm^3/sec$. Denoting the resonances by (n, v, ℓ), the lowest energy resonance structure near 0.01eV is due to (3,4,1), i.e. it is the v=4 level of the $5^2\Sigma^+$ state perturbed by the

311

interference between direct and indirect recombination. The large vibrational spacing in this low reduced mass system allows Rydberg states with both low n and low v to lie above the v=0 level of the ion. While the matrix element in Eq. (3) might be expected to be small because it is a $\Delta v = 4$ transition, this is offset by the low value of n. Moving to higher energies, the (6,1,1) resonance appears with a peak near 0.03eV. The lifetime for predissociation of the resonances can be estimated from the matrix element, (5) $T_{v,d}^{k,\ell}$ in Eq. (5)

$$\tau_{n,v}^{pre} = \frac{\hbar}{\frac{2\pi\rho}{(n-\mu_0)^3} \mid T_{v,d}^{k,\ell} \mid^2}. \tag{9}$$

where μ_0 is the value of the quantum defect at the R value corresponding to the minimum of the ion well.

The lifetimes for predissociation of the (3,4,1) level by the X, A, and C states are $1.0x10^{-9}$, $0.95x10^{-9}$, and $2.6x10^{-13} sec$ respectively. Clearly, the C state is the dominant dissociative route for v=4. In fact, the C state is also the dominant dissociative route for every Rydberg vibrational level. These results are confirmed by the full calculated DR rates at 300K which are $7.7x10^{-12}$, $3.0x10^{-11}$, and $6.6x10^{-9} cm^3/sec$ along the X, A, and C states respectively. Indeed, the plot of the total cross section in Fig. (3) is nearly identical with the cross section for the C state only. The time for a vibration in the $v = 4$ level is given approximately by (15)

$$\tau_v^{vib} = \frac{1}{c(\omega_e - \omega_e x_e - 2v\omega_e x_e)} \tag{10}$$

where c is the speed of light, ω is the fundamental frequency, and $\omega_e x_e$ is the anharmonicity for ^4HeH. Taking the Rydberg state to have the same calculated spectroscopic constants as those for the ion, the lifetime of a vibration is found to be approximately $1.8x10^{-14} sec$. After capture into the (3,4,1) level, the molecule undergoes about 14 vibrations before falling apart. The autoionization lifetime, $\tau_{n,v}^{auto}$, can be calculated approximately from (16)

$$\tau_{n,v}^{auto} = \frac{\hbar}{\frac{2\pi}{(n-\mu_0)^3} \mid \langle v_0 \mid \mu(R) \mid v \rangle \mid^2}. \tag{11}$$

For $v = 4$, the autoionization lifetime is $3x10^{-11} sec$. Therefore, once excited, the (3,4,1) state will almost entirely dissociate.

For ^3HeH and ^4HeH the direct DR cross sections are quite similar with those for ^3HeH slightly larger than those for ^4HeH. However, for the lighter species, the calculated full rate coefficient at room temperature is $2.6x10^{-8} cm^3/sec$. (8) For ^3HeH, the energy difference between vibrational levels is greater than in ^4HeH and a (4,2,1) falls above threshold but is below threshold in ^4HeH. The (4,2,1) level plays a major role in enhancing the ^3HeH DR cross section and rate coefficient over that for ^4HeH.

THE SECOND ORDER ELECTRONIC COUPLING

The indirect mechanism of Bardsley (3) is driven by the Born-Oppenheimer breakdown coupling of Eq. (3). However, it is also possible to have capture into a Rydberg state by an electronic coupling. The first order coupling, in which the electronic Hamiltonian appears once, vanishes between an electron-ion state and a Rydberg state with the same ion core. However, if the Hamiltonian acts twice, using the dissociative state as an intermediate, the electronic coupling can be nonzero. A mechanism involving this type of electronic coupling was first discussed by O'Malley (17) and was used in preliminary calculations on H_2^+ DR by Hickman (18). It was first included in a full MQDT calculation in 1991 (5). The coupling matrix element takes the form

$$\int\int X_v(R)\langle\Psi_v^{k,\ell}\,|\,H(R)\,|\,\Psi_d\rangle F_d(R_<)G_d(R_>)\langle\Psi_d\,|\,H(R')\,|\,\Psi_v^{n,\ell}\rangle X_{v'}(R')dRdR'$$

$$(12)$$

where F_d and G_d are the regular and irregular vibrational wave functions in the dissociative state. An important difference between this mechanism for indirect recombination and the Born-Oppenheimer breakdown mechanism is that we are no longer restricted to the $\Delta v = 1$ propensity rule. A large Δv is possible as long as the initial and final bound vibrational wave functions have a large overlap with the continuum vibrational wave functions of the dissociative state.

The second order mechanism arises from the perturbation expansion of the K matrix in the MQDT approach. (4,5) We have found that the second order mechanism is often more important in some systems than the Born-Oppenheimer breakdown mechanism. In an analysis (5) of the $v = 1$ contributions to the DR cross section for O_2^+ leading to $O(^1S)$ products, we found that the shape of the resonances was due to the interaction between the vibronic and the electronic indirect mechanisms and that the electronic indirect mechanism was dominant. For DR of O_2^+ along the $^1\Delta_u$ route, (19) the cross section near threshold is depressed below the direct cross section by five orders of magnitude due to the electronic indirect mechanism alone and by one order of magnitude due to the vibronic indirect mechanism. Interference between the two processes leads to a full cross section which is three orders of magnitude below the direct cross section. The effect is due to an n=3, v=13 resonance lying 0.02eV below threshold. This level has a wing which interferes destructively with direct recombination above threshold.

The second order coupling is now included in all our calculations involving diabatic electronic couplings. It is clear that in most molecules it must be included in order to calculate accurate cross sections. In molecules having large capture widths, it may be necessary to go beyond second order. Calculations including the full higher order K matrix have been reported by Takagi. (20)

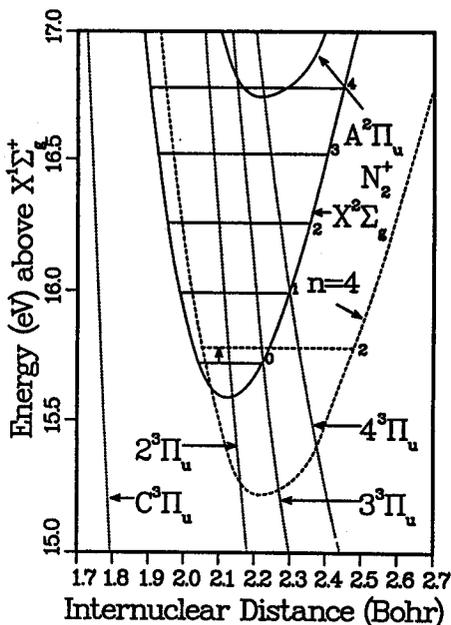In the case of DR proceeding entirely by derivative coupling, as in the

FIG. 4. Indirect recombination through the n=4 $^3\Pi_u$ Rydberg state of N_2 with the excited $A^2\Pi_u$ core. The small vertical arrow indicates capture from the v=0 ion ground state into the (4,2,0) $^3\Pi_u$ state with the $A^2\Pi_u$ core.

previous section, an equivalent second order derivative coupling also can be constructed. In such a coupling for HeH, the initial electron-ion state would be coupled to a Rydberg state by the C state acting as an intermediate. These couplings are all vibronic as opposed to the above electronic couplings. This coupling has not been included in the HeH MQDT calculations to date and will be the subject of future calculations.

EXCITED ION CORE BOUND RYDBERG STATES

Indirect DR through a bound excited core Rydberg state proceeds as shown in Fig. (4) for N_2^+. Because the intermediate Rydberg state does not have the ground state of the ion as the core, it differs from the free electron-ion system in the reactant channel of Eq. (1) by a double excitation, i.e. by moving two electrons to previously unoccupied orbitals. Therefore, the electronic Hamiltonian can drive the capture. The capture matrix element is

$$V_{v,v',\ell,\ell'}^{n^*,k} = \langle \Psi^{n^*,\ell} X_v \mid H \mid \Psi^{k,\ell'} X_{v'} \rangle. \tag{13}$$

This process has been described qualitatively in the literature for DR of N_2^+ (21) and CD^+, (22) but there have been no reported prior calculations. (Note that in the diabatic treatments of H_2^+ DR, all the dissociative routes (23) are excited core Rydberg states but they are all repulsive.) An important

314

qualitative feature of this recombination mechanism is that it is possible to have capture into the $v = 0$ level of excited core states. Such a capture can have large Franck-Condon factors and large capture matrix elements. This type of capture is impossible in the vibronic indirect mechanism since all the $v = 0$ Rydberg levels with the same core as the ion are at lower energies than the ion v=0 level.

We have calculated (25) the effect of intermediate excited core Rydberg levels on the DR of the v=0 level of N_2^+. The relevant potential curves are shown in Fig. (4). The dominant dissociative channels (shown as dotted lines) are the four lowest valence $^3\Pi_u$ states with $2\,^3\Pi_u$ the dominant route for v=0. (24) The calculation includes 18 vibrational levels for the ion ground state and Rydberg states and the four dissociative routes. We have included Rydberg states having the $A^2\Pi_u$ excited core. The inclusion of this state substantially increases the amount of required molecular data and the amount of computer time needed to complete the calculation of cross sections and rates. Since we must treat the A state as well as we treat the X ion core, 18 vibrational levels are also included for the A state and its Rydberg states. In total, the electronic K matrix needed in the MQDT approach includes 36 bound vibrational levels and the four dissociative $^3\Pi_u$ states. In addition, in order to build the K matrix, we need electronic widths for capture of the free electron by the A state into each of the four dissociative states. These widths also give us the predissociation widths of the intermediate A core Rydberg states. We have treated capture of an $\ell = 0, \sigma$ free electron by the $A^2\Pi_u$ ion. Finally, we need the width matrix element of Eq. (13), where the right side describes a "free" electron in the field of the X core and the left side describes a Rydberg state with the A core. The A core lies $0.11a_o$ to larger R than the X core and the minima are separated by only $1.14eV$. The v=0 level of the calculated $n = 3\,^3\Pi_u$ Rydberg state with the A core lies $2.3eV$ below the $v = 0$ level of the $X^2\Sigma_g^+$ state. The first calculated A core Rydberg state above threshold is the $n = 3, v = 11$ state near $0.03eV$ followed by the $n = 4, v = 2$ state near $0.06eV$. The latter level is shown in Fig. (4). The effect of the excited core Rydberg levels is to increase the DR rate by about 10% over the rate calculated with only the four dissociative routes and the ground state ion core Rydberg levels. Note that capture into the $n = 4, v = 2$ level shown in Fig. (4) allows for dissociation along the $4\,^3\Pi_u$ channel which has only small Franck-Condon factors for direct capture from v=0. In this manner, indirect DR can strongly affect the quantum yield of the atomic products. Further details on these calculations will be published separately. (25)

ACKNOWLEDGEMENTS

are both supported by NSF.

REFERENCES

1. D. R. Bates, Phys. Rev. A **78**, 492 (1950).
2. J. N. Bardsley, J. Phys. B **1**, 349(1968).
3. J. N. Bardsley, J. Phys. B **1**, 365 (1968).
4. A. Giusti, J. Phys. B **13**, 3867 (1980).
5. S. L. Guberman and A. Giusti-Suzor, J. Chem. Phys. **95**, 2602 (1991).
6. S. L. Guberman, "Recent Theoretical Developments in Dissociative Recombination," in *Atomic Collisions: A Symposium in Honor of Christopher Bottcher (1945-1993)* (American Institute of Physics Press, New York, 1995).
7. U. Fano, Phys. Rev. **17**, 93 (1978).
8. S. L. Guberman, Phys. Rev. A **49**, R4277 (1994).
9. S. L. Guberman, "The dissociative recombination of $^4HeH^+$", in preparation.
10. G. Sundstrom, S. Datz, J. R. Mowat, S. Mannervik, L. Brostrom, M. Carlson, H. Danared and M. Larsson, Phys. Rev. A **50**, R2806 (1994).
11. J. R. Mowat, H. Danared, G. Sundstrom, M. Carlson, L. H. Andersen, L. Vejby-Christensen, M. af Ugglas, and M. Larsson, Phys. Rev. Lett. **74**, 50 (1995).
12. F. B. Yousif and J. B. A. Mitchell, Phys. Rev. A **40**, 4318 (1989).
13. F. B. Yousif, J. B . A. Mitchell, M. Rogelstad, A. Le Paddelec, A. Canosa and M. I. Chibisov, Phys. Rev. A **49**, 4610 (1994).
14. I. D. Petsalakis, G. Theodorakopoulos, C. A. Nicolaides and R. J. Buenker, J. Phys. B **20**, 5959 (1987).
15. G. Herzberg, *Molecular Spectra and Molecular Structure, I. Spectra of Diatomic Molecules* (Van Nostrand Reinhold Co., New York, 1950), p.98.
16. H. Nakamura, Int. Rev. Phys. Chem. **10**, 123 (1991).
17. T. F. O'Malley, J. Phys. B. **14**, 1229 (1981).
18. A. P. Hickman, J. Phys. B **20**, 2091 (1987).
19. S. L. Guberman, "The dissociative recombination of O_2^+ along the $^1\Delta_u$ route", in preparation.
20. H. Takagi, "Theoretical Problems in the Dissociative Recombination of $H_2^+ + e^-$", in *Dissociative Recombination: Theory, Experiment and Applications,* ed. by B. R. Rowe, J. B. A. Mitchell, and A. Canosa (Plenum Press, New York, 1993), p.75.
21. S. L. Guberman, "Ab Initio Studies of Dissociative Recombination", in *Dissociative Recombination: Theory, Experiment and Applications,* ed. by J. B. A. Mitchell and S. L. Guberman (World Scientific, Singapore, 1989), p.45.
22. P. Forck, C. Broude, M. Grieser, D. Habs, J. Kenntner, J. Liebmann, R. Repnow, D. Schwalm, A. Wolf, Z. Amitay, and D. Zajfman, Phys. Rev. Lett. **72**, 2002 (1994).
23. S. L. Guberman, J. Chem. Phys. **78**, 1404 (1983).
24. S. L. Guberman, Geophys. Res. Lett. **18**, 1051 (1991).
25. S. L. Guberman, "The dissociative recombination of the v=0 level of N_2^{+}", in preparation.

THE PHYSICS OF ELECTRONIC AND ATOMIC COLLISIONS

XIX International Conference

Whistler, Canada July–August 1995

EDITORS

Louis J. Dubé
Université Laval, Québec

J. Brian A. Mitchell
University of Western Ontario, Ontario

J. William McConkey
University of Windsor, Ontario

Chris E. Brion
University of British Columbia, British Columbia